SBAS InSAR Subsidence Monitoring For Mining Areas Based On Levelling Constraints

Zhai Min[1,2] and Liu Qingrong [1] and Tao Qiuxiang [1] and Liu Guolin [1]

[1]College of Geodesy and Geomatics, Shandong University of Science and Technology, Qingdao, Shandong 266590, China;

[2]Qingdao Key Laboratory of Beidou Navigation and Intelligent Spatial Information Technology Application, Shandong University of Science and Technology, China Qingdao 266590, China

Background

The market demand for coal in China is huge, and the ground subsidence, coal mine collapse and natural disasters caused by coal mining have become increasingly serious, which have caused different degrees of impact on people's daily life, ecological balance and sustainable development of the region [1] .Real-time mine surface monitoring is essential to effectively curb accident losses and guide rational mining and mine safety construction.SBAS-InSAR technology analyzes the phase information of multiple interferometric images, deduces the surface deformation rate and DEM error data, and realizes the all-weather acquisition of surface deformation information of the mining area, so as to more comprehensively understand the deformation and subsidence pattern of the mining area.Although SBAS InSAR technology has been widely studied and applied for large-scale monitoring in mining areas[2,3] . However, subject to the influence of spatial and temporal discorrelation, atmospheric delay and noise on the deformation results[4,5] , and the requirements for image quantity, quality, and spatial continuity([6] . Therefore, it has great significance to study the correction of InSAR monitoring results with a small amount of levelling monitoring data as the constraint, so as to achieve the effective improvement of SBAS-InSAR monitoring results accuracy. In this paper, Yuncheng coal mine is selected as the study area, and the subsidence monitoring is carried out in this mine area based on SBAS-InSAR technology. On this basis, the levelling monitoring data is used as the constraint to construct the error surface by quadratic polynomial to correct the SBAS-InSAR monitoring results, and the accuracy level of SBAS-InSAR monitoring is effectively improved.

Methods

For N+1 SAR images at times $t_{0,}t_1,\ldots t_n$ covering the same region, two images that meet the spatio-temporal baseline conditions are selected and combined, and after precise alignment, M interference pairs can be obtained[7] .

$$\frac{N+1}{2} \le M \le \frac{N(N+1)}{2}$$

The highly coherent image elements with stable phase characteristics are selected as the set of highly coherent points and then the phase is unwrapping. In order to make the decoupled differential interferometric phase contain only the deformation phase, the effect of various types of error phases must be removed. Suppose the j-th(j=1,2,…,M) differential interferogram is obtained by doing differential interference between the two scenes of SAR images obtained at t_A and t_B , where the differential interference phase of the high coherent image element at (r,x) is $\delta\phi_j(r,x)$, then

$$\delta\phi(r,x) = \phi(t_B,r,x) - \phi(t_A,r,x) \approx \frac{4\pi}{\lambda}[d(t_B,r,x) - d(t_A,r,x)]$$

where λ denotes the wavelength; $d(t_A,r,x)$ and $d(t_B,r,x)$ denote the cumulative shape variables of the ground surface at the moments t_A and t_B for image element (r,x) relative to the initial moment t_0 upward at Line-of-Sight, then we have

$$\phi(t_A,r,x) = \frac{4\pi}{\lambda}(t_A,r,x), d(t_0,r,x) = 0$$

The time of primary and secondary images be$IE = [IE_1,\ldots.IE_M], IS = [IS_1,\ldots.IS_M]$If, $IE_j > IS_j(j = 1,2,\ldots,M)$then the observation equation consisting of all the differential interferogram phases is

$$\delta\phi_j = \phi\left(t_{IE_j}\right) - \phi\left(t_{IE_j}\right)$$

Then, the linear deformation model of SBAS-InSAR is

$$A\phi = \delta\phi$$

As the matrix A is full rank, the least squares method can be used to solve for the estimate of ϕ

$$\phi = (A^TA)^{-1}A^T\delta\phi$$

Graphics

According to the information of 13 levelling points in the C2 settlement zone from April 2, 2019 to April 15, 2020, the corresponding SBAS monitoring points were selected in C2 and compared with the levelling data, and the point location and point number distribution of the level monitoring points are shown in Figure 1.Table1 shows the difference between the levelling data and SBAS-InSAR subsidence monitoring results, in which the levelling measurement deformation is about 60 cm, and the accumulated deformation of SBAS-InSAR monitoring is about 20 cm.

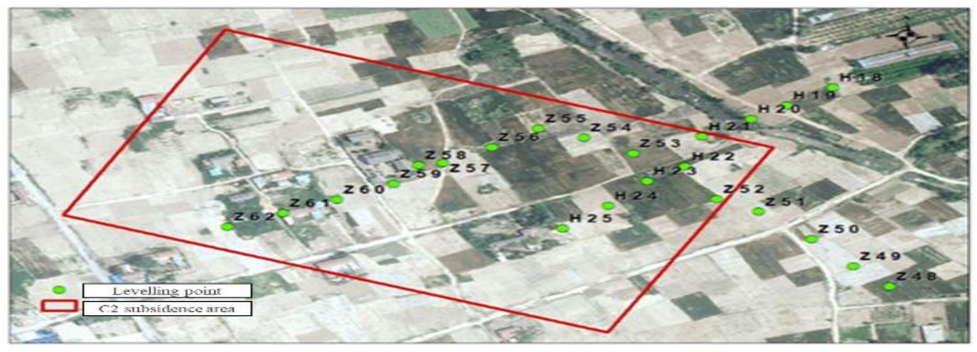

Figure 1:Levelling monitoring point location and point number distribution

Table 1 Subsidence difference between SBAS-InSAR and levelling monitoring (mm/a)

Point Number	Subsidence difference	Point Number	Subsidence difference	Point Number	Subsidence difference
Z48	182.67	Z56	404.37	H19	371.55
Z49	229.27	Z57	403.96	H20	403.05
Z50	274.71	Z58	397.77	H21	413.28
Z51	341.72	Z59	395.32	H22	467.59
Z52	405.74	Z60	401.21	H23	476.59
Z53	446.27	Z61	377.32	H24	416.82
Z54	441.45	Z62	337.36	H25	406.09
Z55	429.52	H18	355.85		

Rsult and discussion

For this reason, the settlement difference based on level and SBAS-InSAR uses quadratic polynomials to construct space surfaces, and the quadratic polynomial surface formula can be expressed as

$$f(x,\ y) = a_{00} + a_{10}x + a_{01}y + a_{11}xy + a_{20}x^2a_{02}y^2$$

Here, x and y are the coordinates of the monitoring points, respectively.

The 17 monitoring points in Table 2 were selected for quadratic polynomial surface construction, and 6 monitoring points (Z52, Z56, Z59, H19, H21, H24) were selected for inspection. The constructed settlement difference quadratic polynomial surface is shown in Figure 4, and the subsidence difference before and after correction is shown in Table 2. It can be seen that the correlation coefficient between the corrected SBAS-InSAR results and the levelling data reaches 0.9286, and the corrected settlement difference RMSE is controlled within ±50 mm/a, and the subsidence monitoring accuracy is improved by more than 90% compared with the pre-correction period, which effectively improves the reliability of the SBAS-InSAR technical results.

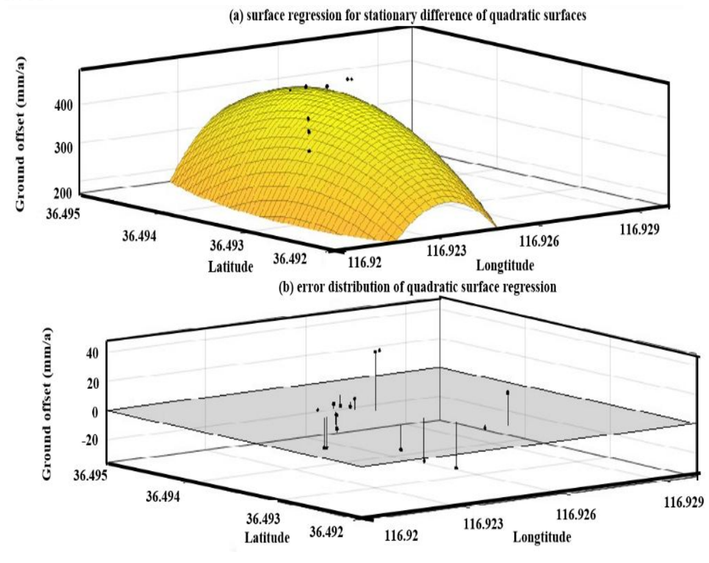

Figure 2: Quadratic polynomial surface fitting

Table 2:Correction of settlement difference statistics (mm/a)

Point number	Before correction	After correction
Z52	405.74	-30.92
Z56	404.37	-29.44
Z59	395.32	-20.42
H19	371.55	3.36
H21	413.28	-38.38
H24	416.82	-41.99
RMSE	401.46	30.24

References

[1] Xu Q. China mine construction of the ecological environment research [D]. Beijing: China University of Mining & Technology,Beijing, 2008. **[2]** Wang Z D, Wen X H, Tang W, et al. Early Detection of Geological Hazards in Longmenshan-Dadu River Area Using Various InSAR Techniques[J]. Geomatics and Information Science of Wuhan University, 2020, 45(03): 451–459.**[3]** Li S, Li Z W, Hu J, et al. Investigation of the Seasonal oscillation of the permafrost over Qinghai-Tibet Plateau with SBAS-InSAR algorithm[J]. Chinese Journal of Geophysics, 2013, 56(05): 1476–1486.**[4]**Xiang W, Zhang R, Liu G, et al. Extraction and analysis of saline soil deformation in the Qarhan Salt Lake region (in Qinghai, China) by the sentinel SBAS-InSAR technique[J]. Geodesy and Geodynamics, 2022, 13(2): 127–137. **[5]** Gabriel A K, Goldstein R M, Zebker H A. Mapping small elevation changes over large areas: Differential radar interferometry[J]. Journal of Geophysical Research Solid Earth, 1989, 94(B7): 9183–9191. **[6]** Li L, Hong Y T. Application of improved SABS technology in monitoring mining land subsidence[J]. Science of Surveying and Mapping, 2020, 45(10): 92–101. **[7]** Berardino P, Fornaro G, Lanari R, et al. A new algorithm for surface deformation monitoring based on small baseline differential SAR interferograms[J]. IEEE Transactions on Geoscience and Remote Sensing, 2002, 40(11): 2375–2383.